Biogeochemistry 3:141–161 (1987)

Big Moose Basin: simulation of response to acidic deposition

GEORGE F. DAVIS[1], JOHN J. WHIPPLE[2], STEVEN A. GHERINI[1], CARL W. CHEN[2], ROBERT A. GOLDSTEIN[3], ARLAND H. JOHANNES[3], PETER W.H. CHAN[1] AND RONALD K. MUNSON[1]

[1]Tetra Tech, Incorporated, 3746 Mt. Diablo Boulevard, Lafayette California, USA
[2]Systech, Incorporated, 3744 Mt. Diablo Boulevard, Lafayette, California, USA
[3]Electric Power Research Institute, 3412 Hillview Avenue, Palo Alto, California, USA

Key words: acidic deposition, Adirondacks, modeling surface water acidification, water chemistry

Abstract. The ILWAS model has been enhanced for application to multiple-lake hydrologic basins. This version of the model has been applied to the Big Moose basin, which includes Big Moose Lake and its tributary streams, lakes, and watersheds. The basin, as defined, includes an area of 96 km^2, with over 20 lakes and ponds, and 70 km of streams. Hydrologic and chemical calibrations have been made using data from seven sampling stations. When total atmospheric sulfur loading to the basin is halved, the model predicts, after four years of simulation, a decreasing sulfate concentration and to a lesser extent a rising alkalinity at Big Moose Lake outlet. At the end of four years, the results show an increase in pH of 0.1 to 0.5 pH units depending upon season.

Big Moose Basin: simulation of response to acidic deposition

Big Moose Lake is the largest acidic lake in the Adirondacks (Colquhoun *et al.*, 1984). The response of this lake and its tributary surface waters to acidic deposition and, in particular, to changes in deposition is of concern. This paper describes an application of the Integrated Lake-Watershed Acidification Study (ILWAS) model to the Big Moose system to predict such responses. It is one in a series of papers on the North Branch of the Moose River discussed in an introductory paper by R.A. Goldstein et al., 1987.

The Big Moose system, as defined here, is the hydrologic basin upgradient of the Big Moose Lake outlet, an area of about 96 square kilometers (Figure 1). The system includes over 20 lakes and ponds (greater than two hectares) and 70 kilometers of streams. The application of the ILWAS model to this entire system, to our knowledge, constitutes the largest lake-watershed acidification simulation performed to date. The simulation of such a large system has become possible because of two critical enhancements made to the ILWAS model during the Regional Integrated Lake-Watershed Acidification Study (RILWAS): 1) improvement of the model's computation speed, and 2) modification of the code to simulate higher order hydrologic systems, in particular those with multiple lakes.

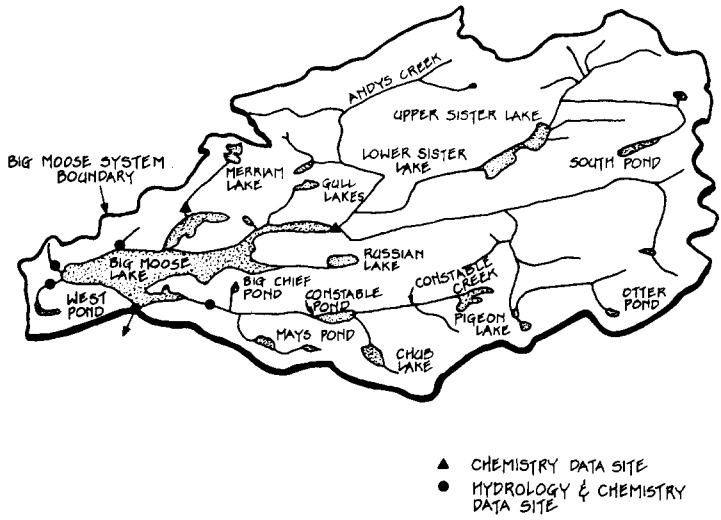

Figure 1. The Big Moose hydrologic system.

This paper first briefly reviews ILWAS model theory. This is followed by a discussion of the above-mentioned model enhancements, the hydrologic and chemical calibration of the Big Moose system, and the simulated response of the system to a reduction in sulfur deposition.

The ILWAS model

The theory and application of the ILWAS model are covered in detail elsewhere (Gherini, Mok, Hudson, Davis, Chen, and Goldstein, 1985; Goldstein et al., 1985; Goldstein, Gherini, Chen, Mok, and Hudson, 1984; Chen, Gherini, Hudson, and Dean, 1984; and Chen, Gherini, and Goldstein, 1979). What follows here is a brief review.

Theory

The ILWAS model was developed to predict changes in surface water acidity given changes in deposition acidity incident to forested ecosystems. The model does this by dividing a lake-watershed system into a network of hydrologic catchments with homogeneous internal compartments (forest canopy, snowpack, soil strata, stream segments, and lake layers). The model routes water from one compartment to another and calculates the concentrations of solutes in the water by simulating the acid-base reactions taking place in each compartment.

The hydrologic routing is accomplished by simulating 1) the fraction of precipitation which is rain and snow, 2) liquid interception by the forest canopy, 3) evapotranspiration, 4) snowpack accumulation and melting, 5) vertical and lateral flow through soil layers, 6) stream flow, 7) vertical

distribution of lake inflow and outflow, and 8) lake volumetric discharge.

Simple empirical formulations are used to represent items 1, 2, 3, 4, and 8 above. Routing of water through the soil layers is simulated using the continuity equation and the Darcy equation for vertical and lateral seepage, with the unsaturated hydraulic conductivity assumed to vary linearly with soil moisture content between field capacity and saturation. Stream flow is simulated by Muskingum routing (Linsley, 1975). Lake discharge is computed by solving an overall water balance equation for the lake simultaneously with a lake-stage discharge relationship. Surface water inflows to the lake are routed to a layer of equal density; ground water seepage is mixed with the layer adjacent to its point of entry. Water discharged from the lake comes primarily from the surface. Depending upon the degree of density stratification and the lake discharge rate, deeper water may be entrained in the outflow.

The density stratification is determined from the water temperature and its solute content. Water temperature is determined from a lake heat budget which includes terms for long and short wave solar radiation, back radiation, and evaporative, conductive and advective heat transfers. Latent heats associated with the formation and melting of lake ice are also considered.

To simulate pH, the ILWAS model tracks total alkalinity (Alk, also called acid neutralizing capacity, ANC), total inorganic carbon (TIC), total monomeric aluminum (Al_T), and total organic acid (R_T). Because the measurement of pH only quantifies those hydrogen ions free in solution (e.g., as $H_9O_4^+$, rather than as, say H_2CO_3), the calculation of pH by mass balancing free hydrogen ions in solution is in most cases impossible. Instead, pH can be evaluated implicitly from Alk, TIC, Al_T, and R_T. The model simulates total alkalinity by separately following the alkalinity associated with water, the carbonate system, organic acids, and aqueous aluminum.

Alkalinity can be calculated as the difference between the sum of the concentrations of hydrogen ion acceptors minus hydrogen ion donors, relative to a proton reference level (Stumm, 1970, 1981), e.g.,

$$\begin{aligned} \text{Alk} = {} & [HCO_3^-] + 2[CO_3^{2-}] + [\text{other hydrogen ion} \\ & \text{acceptors, for example, } Al(OH)_2^+ \text{ and } Al \cdot R] - \\ & [H^+\text{-ion donors}] \end{aligned} \tag{1}$$

where

HCO_3^- = bicarbonate ion
CO_3^{2-} = carbonate ion
$Al \cdot R$ = aluminum-organic acid complex, and
[ ] = concentrations, in moles per liter.

Alternatively, alkalinity can be approximated as the difference between the

sum of the analytical totals of the base cations, including aluminum, times their uncomplexed charge at the equivalence point, minus the analytical totals of the strong acid anions, times their uncomplexed charge at the equivalence point (Gherini, et al., 1985):

$$\text{Alk} = \sum_{i=1}^{n} |Z_i| \, C_{T_i} - \sum_{j=1}^{m} |Z_j| \, A_{T_j} \tag{2}$$

where

C_{T_i} = total analytical concentration of cationic constituent i, whose predominant uncomplexed species has a charge, Z_i at the equivalence point, and

A_{T_j} = total analytical concentration of anionic constituent j, whose predominant uncomplexed species has a charge, Z_j at the equivalence point.

In natural waters, the sums on the right-hand side of Equation (2) can be represented as,

$$\sum_{i=1}^{n} |Z_i| \, C_{T_i} = 2[Ca_T] + 2[Mg_T] + [K_T] + [Na_T] + [NH_{4_T}] + 3[Al_T], \tag{3}$$

and

$$\sum_{j=1}^{m} |Z_j| \, A_{T_j} = 2[SO_{4_T}] + [NO_{3_T}] + [Cl_T] \tag{4}$$

where the subscript "T" stands for the analytical total. In equation 3, multiplying the total monomeric aluminum by 3 is equivalent to setting the alkalinity proton reference level (Stumm, 1970, 1981) to include Al^{3+}. The other proton reference level species include H_2O, aqueous CO_2, and fully protonated organic acid. Alternate reference levels can also be selected and used in the ILWAS model, since all major ions are tracked explicitly as opposed to tracking a composite representation (e.g. alkalinity alone). Alkalinity as treated mathematically in Equations 3 and 4 is referred to as C_B–C_A alkalinity. The derivation of Equation (2) has been previously presented (Gherini et al., 1985). Alkalinity calculated using Equation (2) has been shown to be comparable with Gran titrated alkalinity (Schofield et al., 1985) for low dissolved organic carbon waters.

In the ILWAS model, alkalinity, TIC, Al_T, and R_T are all transported using mass balance techniques as are the components of C_{T_i} (e.g., Ca_T) and A_{T_j} (e.g., NO_{3_T}). The H^+-ion concentration (or pH) is calculated implicitly using numerical procedures from an expression giving alkalinity as the sum of its components. The expression is of the form

Table 1. Solution phase chemical constituents simulated by the ILWAS model*

Cations	Anions	Uncharged species	Analytical total	Gases (deposition only)
Ca^{2+}	SO_4^{2-}	H_4SiO_4	Alk[ANC]	(SO_x)
Mg^{2+}	NO_3^-	$CO_2(Aq)$	Org Acid 1	(NO_x)
K^+	Cl^-	AlF_3	Org Acid 2	
Na^+	$H_2PO_4^-$	AlR_1	Al_T	
NH_4^+	F^-	$Al(R_2)_3$	C_T(DIC)	
H^+	$Al(OH)_4^-$	$Al(OH)_3^0$	F_T	
Al^{3+}	HCO_3^-	H_3R_1		
$Al(OH)^{2+}$	CO_3^{2-}	HR_2		
$Al(OH)_2^+$	R_1^3			
AlF^{2+}	HR_1^{2-}			
AlF_2^+	$H_2R_1^-$			
$Al(SO_4)^+$	R_2^-			
AlR_2^{2+}	AlF_4^-			
$Al(R_2)_2^+$	AlF_5^{2-}			
	AlF_6^{3-}			
	$Al(SO_4)_2^-$			

*Mass balance principles are applied to those constituents shown in regular type. Constituents shown in italics are derived from the former using solution phase equilibrium expressions.

Table 2. Physical-chemical processes simulated by the ILWAS model

Canopy processes
Dry deposition
Foliar exudation
Nitrification
Solution phase equilibration
Washoff

Snowpack processes
Accumulation
Sublimation
Leaching
Nitrification

Soil processes
Heat transfer
Biomass loop
  Litter accumulation
  Litter decay
  Organic acid decay
  Nitrification
  Nutrient uptake (tree growth)
  Root respiration
Abiotic processes
  CO_2 exchange
  Competitive cation exchange (Ca, Mg, K, Na, NH_4, H)
  Anion adsorption (SO_4, PO_4, organic acid)
  Mineral weathering (up to 5 minerals)
  Aluminum dissolution — precipitation
  Solid–Liquid–Gas phase equilibration

Surface water processes
Gas transfer
Mixing (advection & dispersion)
Heat exchange
Ice formation
Algal nutrient uptake
Nitrification
Reductive loss of strong acid anions
Solution phase equilibration

$$\text{Alk} = \text{TIC}' \sum_i i \cdot \alpha_{C_i} + R_T' \sum_k k \cdot \alpha_{R_k} + Al_T' \sum_j j \cdot \alpha_{Al_j} + \text{similar terms for complexes} \quad (5)$$

where the $'$ symbol stands for the uncomplexed totals, and the α's are ionization constants (Butler, 1964). The latter are functions of pH and temperature alone. For example, for the aqueous carbonate system, α_{C_1} is

$$\alpha_{C_1} = \frac{HCO_3^-}{\text{TIC}'} = \left(\frac{1}{([H^+]/K_{C_1}) + 1 + (K_{C_2}/[H^+])}\right) \quad (6)$$

where

$[H^+]$ = the free hydrogen ion concentration, and

$K_{C_{1,2}}$ = the first and second dissociation constants for $H_2CO_3^*$.

For the model's triprotic organic acid analogue, α_{R_1}, is

$$\alpha_{R_1} = \frac{[H_2R^-]}{R_T'} = \left(\frac{1}{([H^+]/K_{R_1}) + 1 + (K_{R_2}/[H^+]) + (K_{R_2}K_{R_3}/[H^+]^2)}\right) \quad (7)$$

where

$K_{R_{1,2,3}}$ = the first, second, and third acid dissociation constants for the organic acid analogue.

For aluminum, α_{Al_1} is

$$\alpha_{Al_1} = \frac{Al(OH)^{2+}}{Al_T'} = \left(\frac{1}{([H^+]/K_{Al_1}) + 1 + (K_{Al_2}/[H^+]) + (K_{Al_2}K_{Al_3}/[H^+]^2) + (K_{Al_2}K_{Al_3}K_{Al_4}/[H^+]^3)}\right) \quad (8)$$

where

$K_{Al_{1,2,3,4}}$ = the first, second, third, and fourth hydrolysis constants for aqueous monomeric aluminum.

The chemical species to which conservation of mass principles are applied (i.e., those that are tracked) are shown in regular type in Table 1, along with those species which can be derived from them (italics).

The processes shown in Table 2 are explicitly simulated by the ILWAS model. Several add acid or base to the water flowing through the hydrologic basin. Both rate (time dependent) and equilibrium (time independent) processes are included.

Model code

The 14,000 line code for the ILWAS model was originally written in FORTRAN 66. Versions are available in both FORTRAN 66 and FORTRAN 77. The model has been run on PRIME, IBM, CDC, DEC, and Cray computers. Execution time for a hydrologic basin of moderate complexity (8 catchments) with a single lake ranges from about 20 seconds per simulation year on the Cray 1A (D. Grigal, personal communication) to about 130 minutes per simulation year on the PRIME 550-II.

Model enhancements

Several enhancements to the ILWAS model have been made during the RILWAS project, including alternate provisions for simulation of aqueous inorganic carbon concentrations and soil temperature, and a procedure for simulating reduction reactions for sulfate. Two major enhancements improved the computation speed and allowed simulation of hydrologic basins with multiple lakes. These are described briefly below:

Accelerated Convergence Algorithm

Among the 41 subroutines in the model, the one most frequently called, PHALKN, also requires the bulk of the total computational effort. This routine calculates the H^+-ion concentration (or pH) from alkalinity (ANC), TIC, Al_T, and R_T using an interactive solution technique. The development of the accelerated convergence algorithm reduced the number of iterations needed and therefore the computer time. Since the subroutine is used in the equilibrium calculations for throughfall, soil layer solutions, and stream and lake water, the time savings is substantial. Computer time requirements are only about one-third of what they were previously.

The new convergence algorithm is used to solve Equation (5). It starts by determining two trial values of the H^+-ion concentration, $[H^+]_1$ and $[H^+]_2$, which yield values of ERROR (the difference between the calculated alkalinity and the known, or tracked, value of alkalinity, $ERROR_1$ and $ERROR_2$) with different signs (Figure 2). An initial guess of the correct H^+-ion concentration, $[H^+]_3$ and its associated $ERROR_3$, is then made using the secant method (Carnahan, 1969). Lines and intercepts with the horizontal axis and are determined which pass through $ERROR_3$ and the two initial ERROR values ($ERROR_1$ and $ERROR_2$). A new guess of the correct H^+-ion concentration, $[H^+]_4$, is determined by a weighted average of the two intercepts, and at the same time, the interval is made smaller by moving the endpoint with the same sign as $ERROR_3$ ($ERROR_2$ in this case) inward. These steps are repeated until the absolute value of ERROR is smaller than a user-specified tolerance.

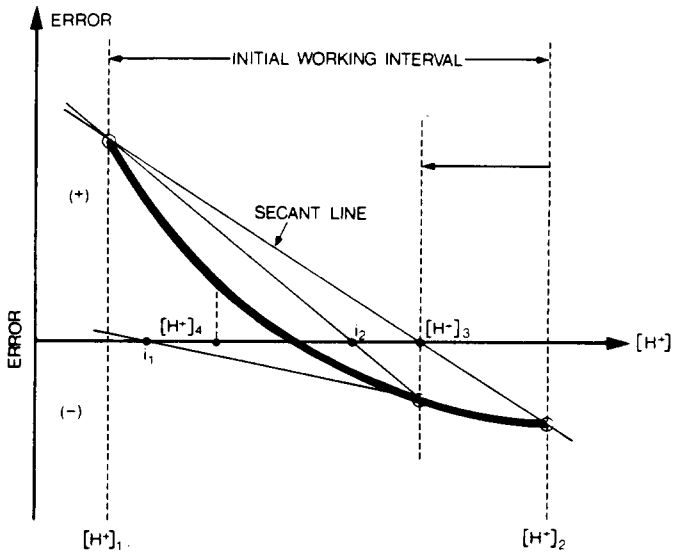

Figure 2. Numerical convergence procedure.

Higher order hydrologic basins

The original version of the ILWAS model could only simulate streams or single lake hydrologic basins, thus limiting applications to headwater systems. To directly handle multiple lake systems such as those found on the North Branch of the Moose River, an extension to the model code was necessary. Two approaches were considered: 1) to extend the dimensions of the code to allow simultaneous simulation of multiple lakes during a single model run, and 2) to sequentially cascade the results from upstream systems downstream, much in the manner the model routes water within a single lake basin. The latter method (cascading) was chosen for two reasons. First, the problem size is not restricted by computer memory limitations. The output of an upstream basin is temporarily stored and then used during the simulation of the next downstream system. A large system can thus be divided into several smaller ones without sacrificing the level of discretization desired. Also the model will continue to be usable on medium-size computers (i.e., mini's). Second, the cascading approach allows a user to calibrate the model in steps, moving from upstream to downstream systems.

Model application

Basin Discretization

The Big Moose Lake drainage system is illustrated in Figure 1. Figure 3 indicates a division of the Big Moose drainage system into four sub-basins.

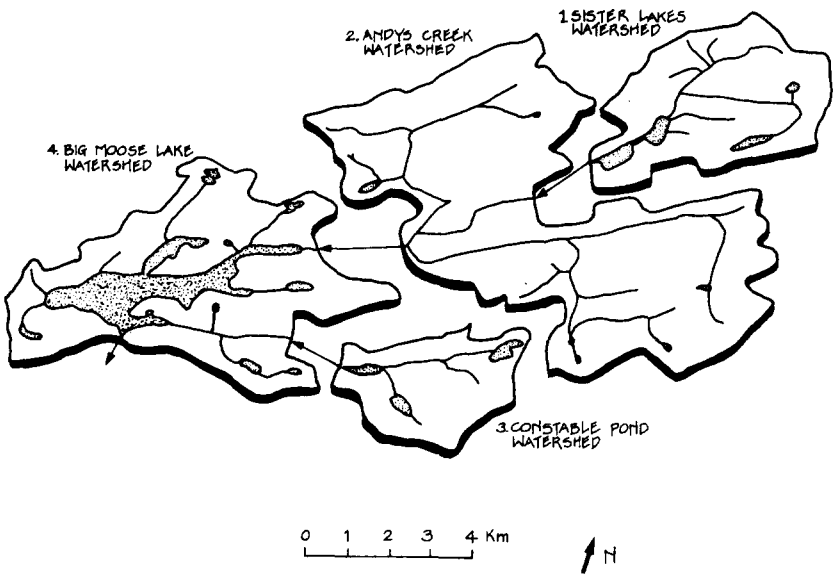

Figure 3. Division of the Big Moose drainage system into four sub-basins.

These sub-basins form a network of watersheds. All sub-basins directly or indirectly feed into Big Moose Lake, which is furthest downstream in the system.

Not all lakes in the Big Moose system are simulated directly as lakes. By simulating the smaller ones as stream segments, the number of sub-basins required to model the entire system is reduced. Lakes which are simulated as stream segments include those which have short hydraulic detention times, and relatively small surface areas, (e.g., Otter Pond). In these cases, treating the lakes as stream segments will have little effect on the simulation results as compared to simulating them as lakes. Another case where a lake might be simulated as a stream segment is when the lake and its watershed represent only a small fraction of the drainage area above hydrologic and chemical calibration points (e.g., South Pond has a watershed area which covers only two percent of the total drainage area above the Andys Creek sampling site). In these cases, the lakes' effects on the volumetric discharge and solute concentrations at the calibration points are minimal.

Hydrologic Calibration

The hydrologic calibration procedure for the ILWAS model has been described elsewhere (Gherini et al., 1985). The first step typically involves adjusting the basin evapotranspiration such that the cumulative volumetric lake outflow over an integration period is close to that observed. Seasonal variations in flow are accommodated by making changes in the snow formation and melting temperatures and the seasonal evapotrans-

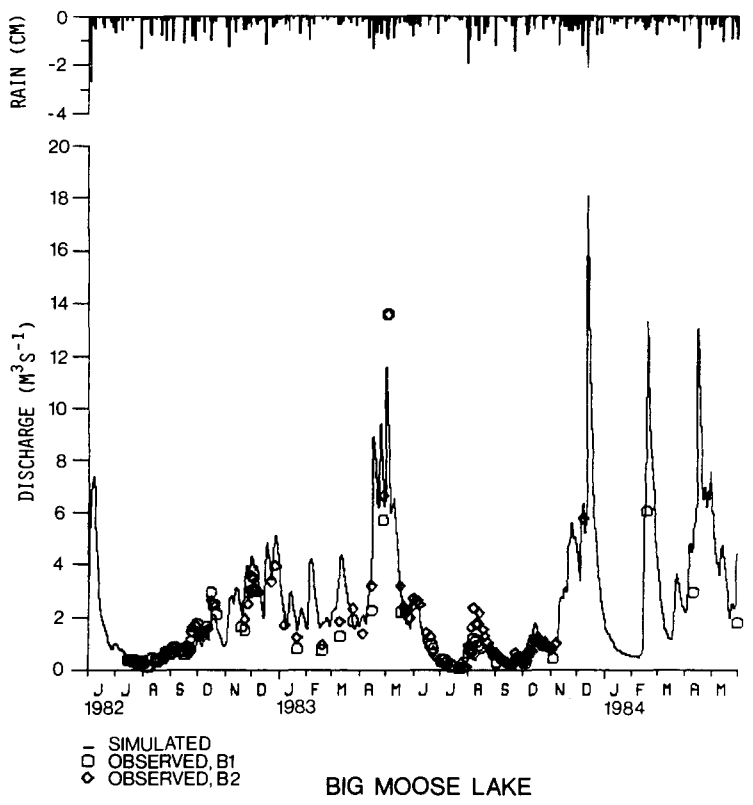

Figure 4. Simulated and observed instantaneous discharge at Big Moose Lake outlet.

piration coefficients. The routing of lateral flows through the various soil layers is calibrated to obtain an acceptable fit to the stream and lake instantaneous discharge data. This is done by making small changes to the soil hydraulic conductivity and field capacity (gravimetric water content).

Meteorological data required to drive the model for the Big Moose basin are available from three stations (BMA, BMN, and Old Forge). The soils of the Big Moose basin have similar characteristics to those previously studied in Woods Lake watershed. For this reason, some of the hydrologic parameters for Big Moose basin have been estimated from values measured for Woods Lake soils.

Soil and till depths have been estimated from surficial geology maps of the Big Moose basin (Newton et al., 1987). Much of the basin is comprised of thin till (less than three meters deep). Forest cover and canopy distributions have been estimated from tree surveys and aerial photos (Cronan et al., 1986). Monthly leaf area indices and soil moisture parameters (field capacities and saturated moisture contents) are the same as used for Woods Lake. Lake volumes are derived from bathymetric maps (C.T. Driscoll, personal communication). Soil permeabilities and evapotrans-

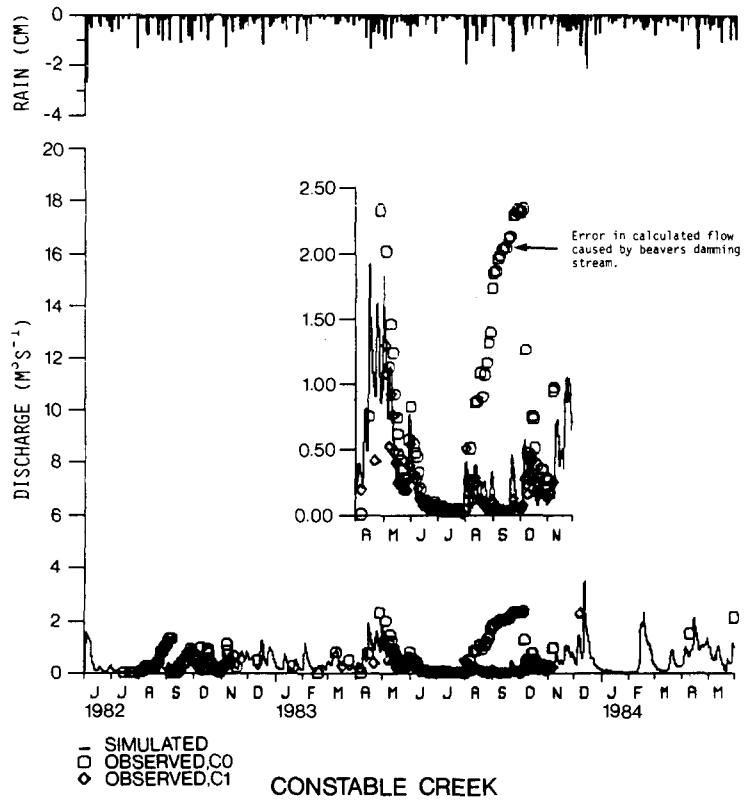

Figure 5. Simulated and observed stream flow for Constable Creek. Gauging stations are located just upstream of entry point to Big Moose Lake. Insert is a vertical magnification of the larger plot for the period April through November 1983. The insert shows erroneous discharge values due to high surface water elevations caused by beavers damming the stream immediately below station "CO".

piration parameters were varied slightly from those used for the Woods Lake basin to better simulate stream discharge dynamics.

In Figure 4, the mean daily simulated outflow for Big Moose Lake is compared to the instanteous discharge estimates obtained from staff gauges installed near the lake outlet. Figure 5 compares simulated and staff gauge derived stream flows for Constable Creek at a location slightly upstream of its entry point to Big Moose Lake. Together Constable Creek and Andys Creek supply approximately 70 percent of the inflow to the lake.

The observed volumetric flows are obtained by converting staff gauge readings to discharge based on stage-flow rating points. In this particular study, however, beaver activity has rendered some of the staff gauge readings of limited value. The insert in Figure 5 enlarges the hydrograph for Constable Creek for the period April to November, 1983. Flow estima-

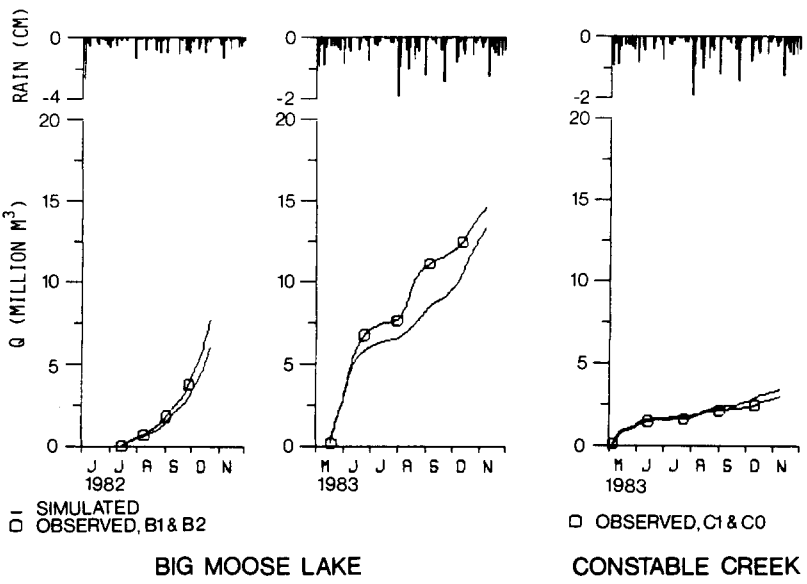

Figure 6. Comparison of simulated and observed cumulative discharge for Big Moose Lake outlet and Constable Creek.

tes were obtained from water levels recorded by two staff gauges (BMC0 and BMC1) located approximately 150 meters apart on the creek. The gauge at station BMC0 recorded high water levels, and hence indicated a period of high flow, during the months of August and September. The gauge at station BMC1, however, recorded low water levels, and hence indicated a period of low flow, during the same months. These were actually low-flow months, but a dam built by beavers downstream of station BMC0 caused local ponding of the creek, and thus resulted in high water levels being recorded on the staff gauge even though the stream flow was low (Peters and Driscoll, 1987).

The simulated and observed cumulative runoff for various periods at the Big Moose Lake outlet and at Constable Creek are compared for periods with sufficient field data (Figure 6). Figure 6 indicates that the cumulative discharges during these times are simulated within ten to twenty percent of the observed values.

The simulated lateral flows through the Big Moose basin soils are summarized in Figure 7. The relative amounts of lateral flow entering the surface waters of the basin from deep ground water flow and from shallow subsurface flow (interflow) are shown. The simulated amount of precipitation falling directly onto surface waters is also shown for comparison. Most of the water enters the surface water system as shallow subsurface flow.

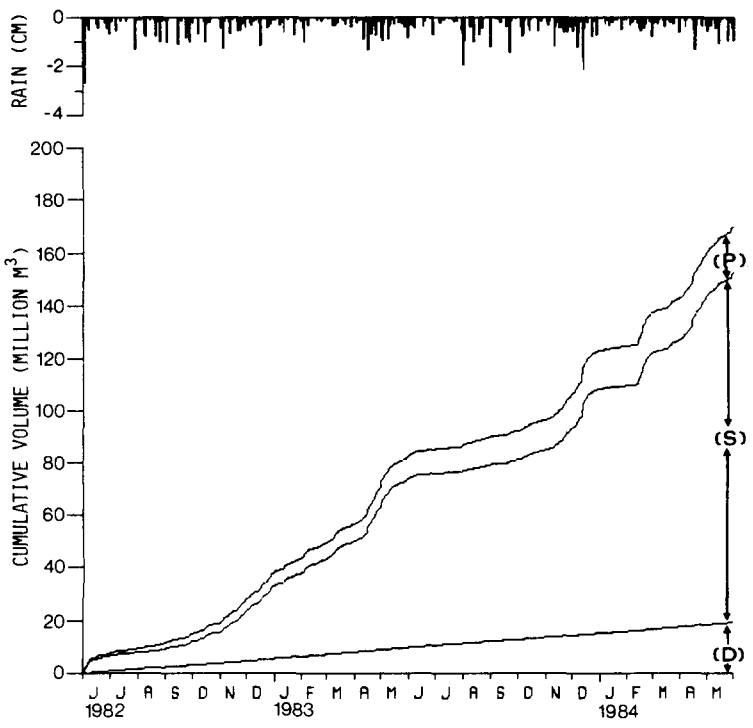

Figure 7. Sources of input to surface waters. P = direct precipitation, S = shallow lateral seepage through soils (interflow), D = deep lateral seepage through soils.

Chemical Calibration

The procedure for chemical calibration has been described by Gherini et al., 1985. In summary, calibration starts with preparing the time-invariant chemical data input file, which includes establishing the initial surface and ground water concentrations. Adjustments of the ion exchange selectivity coefficients, the nitrification, gibbsite solubilization, and mineral weathering rate coefficients are then made to bring the simulated concentrations into agreement with the observed data.

For model calibration, daily atmospheric input data were taken from the BMA meteorological station located within the Big Moose basin. Over the two year period of record, precipitation amount averaged 130 cm/yr and volume weighted average concentrations were as follows: C_B = 31 μeq/l, C_A = 82 μeq/l, and sulfate = 50 μeq/l.

Water quality calibration data for the Big Moose basin are available at four locations (Driscoll et al., 1987): at the outlet of Andys Creek, which

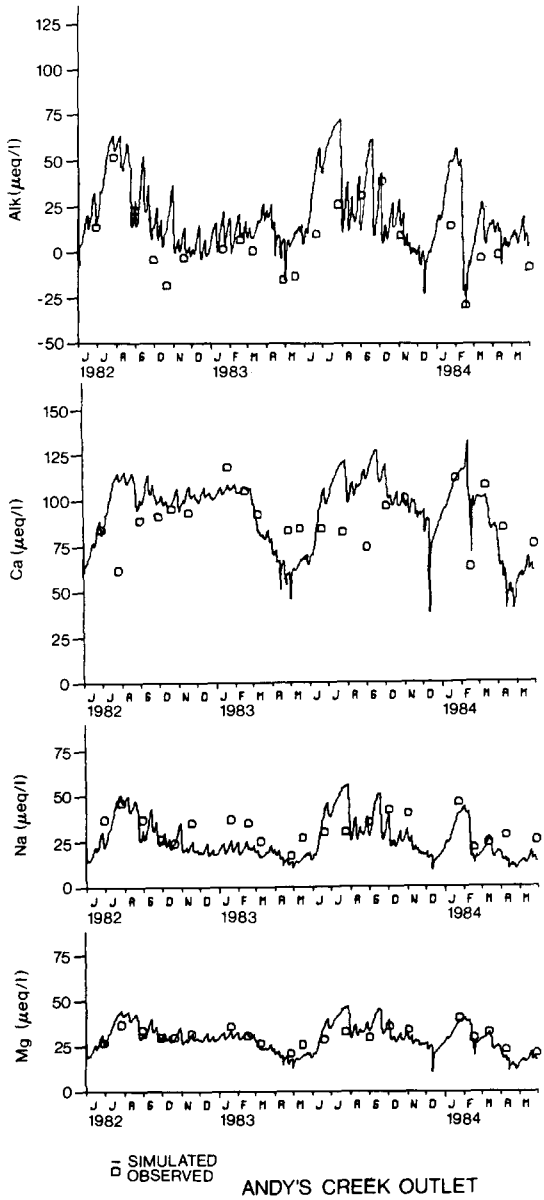

Figure 8. Andys Creek: Simulated and observed alkalinity, calcium, magnesium, and sodium concentrations.

feeds directly into Big Moose Lake; along Constable Creek, a short distance upstream of its outlet into Big Moose Lake; along the outlet stream from Merriam Lake, near its inlet to Big Moose Lake; and at the outlet of Big Moose Lake itself (Figure 1). Calibration data are not

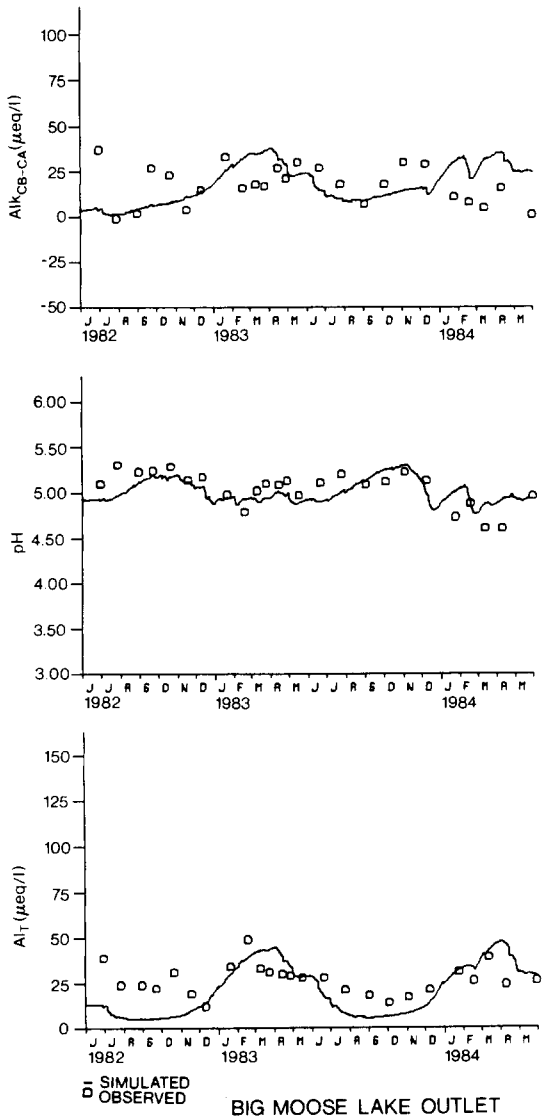

Figure 9. Big Moose Lake outlet: Simulated and observed alkalinity, pH, and total monomeric aluminum.

available for the Sister Lake watersheds, but the water quality at the outlet of lower Sister Lake would be expected to be similar to the water quality at the outlet of Andys Creek.

The Andys Creek subsystem appears to contribute much of the alkalinity input to Big Moose Lake. The predicted alkalinity, calcium, mag-

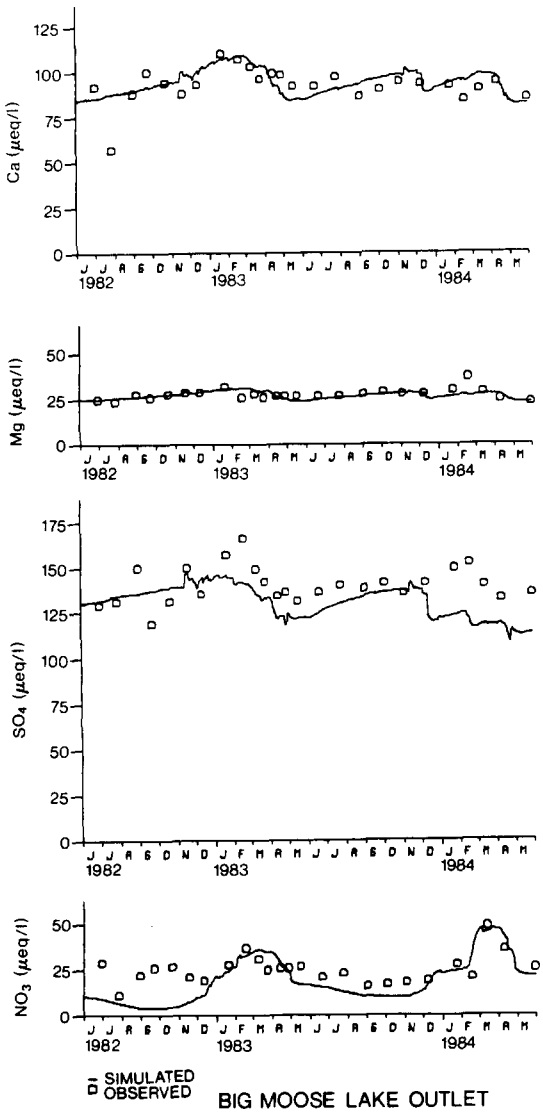

Figure 10. Big Moose Lake outlet: Simulated and observed calcium, magnesium, sulfate, and nitrate concentrations.

nesium and sodium concentrations for Andys Creek are plotted with the observed data in Figure 8. The simulated and observed alkalinity, pH, total monomeric aluminum, calcium, magnesium, sulfate, and nitrate for the Big Moose Lake outlet are plotted in Figures 9 and 10.

It should be noted that at the alkalinity values encountered (e.g., ≈ 0), small errors in alkalinity can cause large changes in pH. For example, for

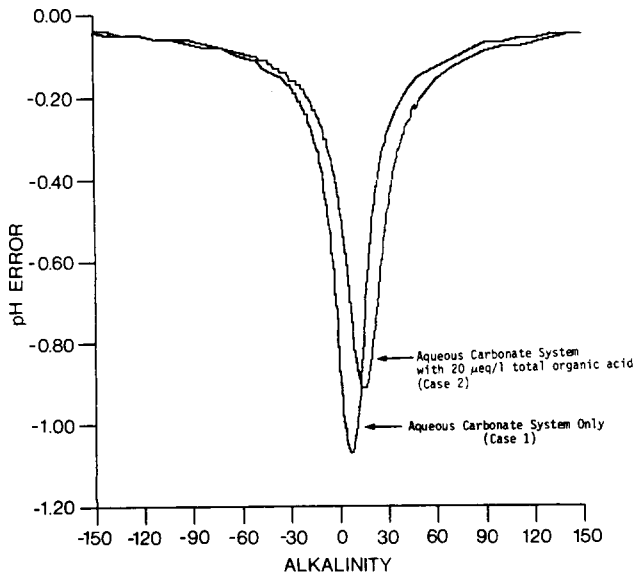

Figure 11. The error which will occur in pH if alkalinity is underestimated by 15 μeq/l, when the true alkalinity is zero. For example, if the true alkalinity was 0.0 μeq/l and the erroneous alkalinity was − 15 μeq/l, the resulting pH error would be about − 0.9 units for a system with R_T = 20 μeq/l.

waters with alkalinities between − 30 and + 30 μeq/l, a 15 μeq/l error in alkalinity would have a large effect on any calculated pH values. The effect of such an error is shown in Figure 11 for water without (Case 1) and with (Case 2) organic acid. At zero alkalinity, a 15 μeq/l error in alkalinity would lead to about a one unit error in pH.

With a complete water quality data set, it is possible to use the data to make internal checks of the data's consistency. For example, alkalinity may be determined as shown previously in Equation (2) (C_B–C_A alkalinity) and then compared with the titrated (Gran) alkalinity. In calculating C_B, it was found that for 15 out of 27 samples no data were available for ammonium ion concentration. Where such data were missing, a value of 5 μeq/l was assumed, corresponding to the average value of the reported ammonium ion concentrations (measured values ranged from 0 to 11 μeq/l). Figure 12a compares the C_B–C_A alkalinity and the titrated alkalinity for Big Moose Lake. The C_B–C_A alkalinity is almost always greater than the titrated values. The average difference between the two for Big Moose Lake is + 16.5 μeq/l.

The cause of this difference has not been resolved. The difference could result from curvature, due to organic acids, in the strong acid portion of the titration curve to which the F_1 Gran function is fitted. It could also result from a systematic positive error in the measurement of the cations

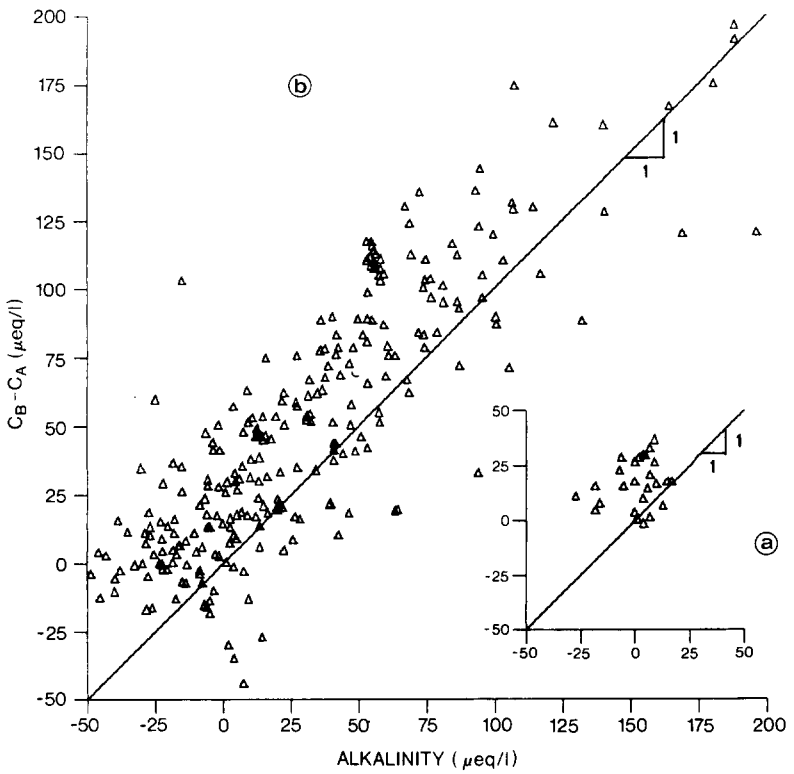

Figure 12. C_B–C_A alkalinity versus titrated alkalinity a) for the Big Moose Lake outlet; b) C_B–C_A alkalinity versus titrated alkalinity for all the RILWAS lakes and streams.

and/or a negative error in the measurement of the anions. Deviations in the charge of Al_T from 3+ at the Gran equivalence point may also influence the results for samples with high aluminum concentrations. Still another possibility may be the presence of relatively strong organic acids which are still essentially unprotonated at the titration equivalence point. Differences between C_B–C_A alkalinity and Gran titration alkalinity are seen in data for the other RILWAS watersheds (Figure 12b) and for data taken by other investigators for different systems (Schofield, 1985). Recent data indicate that in high DOC waters from upstate Minnesota (DOC $\approx$ 15–20 mgC/l), Gran alkalinities can be 60–90 μeq/l less than C_B–C_A alkalinities (total monomeric aluminum concentrations in these waters were less than 5 μmol/l, C.T. Driscoll, personal communication). At alkalinity values near zero, it is necessary to give equal consideration to both the observed alkalinity *and* pH during model calibration.

Simulated response to a halving in total sulfur deposition

To predict the response of the Big Moose system to changes in atmospher-

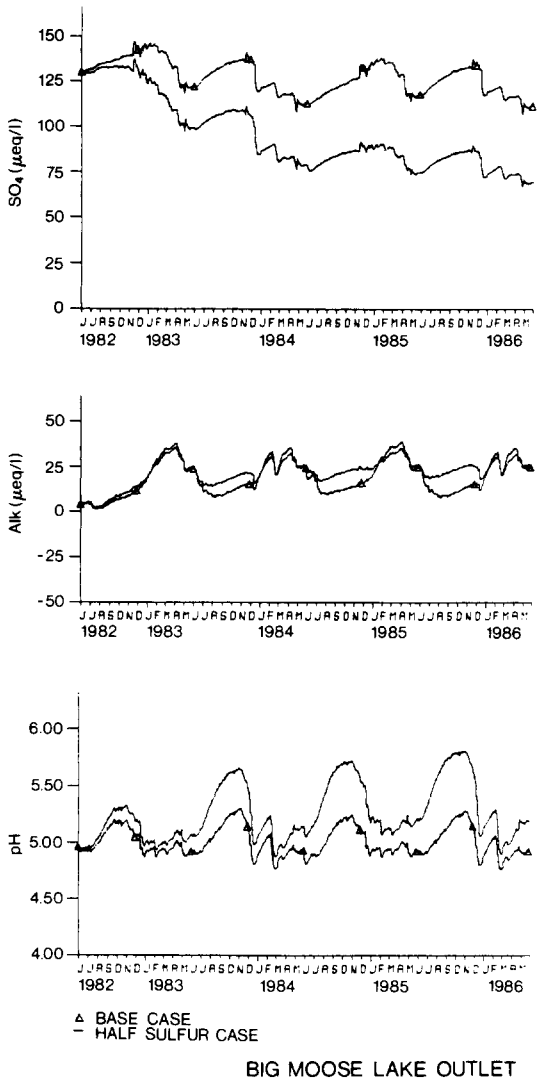

Figure 13. Simulation fo the response of Big Moose Lake outlet water quality to a halving in sulfur deposition.

ic sulfur loadings, we have simulated an arbitrary halving of the total atmospheric sulfur loading to the entire Big Moose system. The other atmospheric loadings were held constant. It should be noted, however, that field data indicate that when the concentration of sulfate in deposition is low, so too are the concentrations of the base cations and the other acid anions. The overall effect of this might be a lessening of the increase in alkalinity and pH of the deposition if sulfur levels were actually halved. The results of the simulation when sulfur alone was halved are presented

in Figure 13 for a four-year period. The results for both the base case and halved sulfur loading are shown for sulfate, alkalinity, and pH. The simulations were made using the two years of observed meteorological data twice to create the four-year simulation period.

By halving the sulfur loading, the sulfate concentration at the Big Moose Lake outlet decreases and the alkalinity increases, but to a lesser extent, due to decreases in the mobilization of base cations. Although the alkalinity change is small, at these low alkalinity values the model predicted a 0.1 to 0.5 pH unit increase during the fourth year of simulation.

By the end of the fourth year of simulation the Big Moose system had not reached a dynamic steady state. In the simulated response of Woods Lake to a halving in the sulfur load, the system had approached a dynamic steady-state within about four years (Gherini et al., 1985). In the much larger Big Moose system (cf. 96 km^2 versus 2 km^2 for Woods), the time to reach a dynamic steady-state is longer and thus requires a longer simulation.

Summary

The ILWAS model, modified to simulate multiple lake systems and using an accelerated numerical solution technique, has been applied to the system of lakes and streams which comprise the Big Moose Lake drainage basin. Hydrologic and chemical calibration results show agreement with the observed data.

Using the calibration of the Big Moose system, the effect of a halving of the total sulfur loading has been evaluated for a four-year period. At the end of the four-year period, the simulated sulfate concentration at the Big Moose Lake outlet had decreased and to a lesser extent the simulated alkalinity had increased. The simulated pH also had increased by about 0.1 to 0.5 pH units depending upon season. At the end of the four-year simulation period, the lake outlet sulfate concentration, alkalinity and pH were still changing. A longer simulation would be required in order for the system to reach a dynamic steady-state.

Acknowledgements

The authors would like to thank the Electric Power Research Institute and the New York Power Pool (ESEERCO) for funding this work. We would also like to thank the RILWAS investigators for providing data and process insights. RILWAS investigators include Elmar Altwicker, Christopher Cronan, Robert Newton, Richard April, Norman Peters, Charles Driscoll, and Carl Schofield. We would also like to thank Trudy Rokas and Susan Callaway of Tetra Tech for typing this manuscript.

References

Butler, J.N. 1964. Ionic Equilibrium a Mathematical Approach. Addison-Wesley Publishing Company, Inc., Reading, MA.

Butler, J.N. 1982. Carbon Dioxide Equilibria and Their Applications. Addison-Wesley Publishing Company, Inc., Reading, MA.

Carnahan, B., H.A. Luther, J.O. Wilkes. 1969. Applied Numerical Methods. John Wiley and Sons, New York, New York.

Chen, C.W., S.A. Gherini, and R.A. Goldstein. 1979. Modeling the Lake Acidification Process. In Proceedings of Workshop on Ecological Effects and Acid Precipitation. Central Electricity Research Laboratory, United Kingdom. Section 5, pp. 1–26.

Chen, C.W., S.A. Gherini, R.J.M. Hudson, J.D. Dean. 1984. The Integrated Lake-Watershed Acidification Study, Volume 1: Model Principles and Application Procedures. Electric Power Research Institute, RP1109-5, EA-3221.

Colquhon, J., W. Kretser and M. Pfeiffer. 1984. Acidity status update of lakes and streams in New York State. New York State Department of Environmental Conservation Report, WM P-83 (6/84), 49 pp., Albany, NY.

Cronan, C.S., J.C. Conlan, and S. Skibinski. 1987. Forest Vegetation in Relation to Surface Water Chemistry in the North Branch of the Moose River, Adirondack Park, NY. Biogeochemistry 3:121–128.

Driscoll, C.T., C.P. Yatsko, and F.J. Unangst. 1987. Longitudinal and Temporal Trends in the Water Chemistry of the North Branch of the Moose River. Biogeochemistry 3:37–61.

Gherini, S.A., L. Mok, R.J.M. Hudson, G.F. Davis, C.W. Chen, R.A. Goldstein. 1985. The ILWAS Model: Formulation and Application. Water, Air, and Soil Pollution 26:425–459.

Goldstein, R.A., S.A. Gherini, C.W. Chen, L. Mok, and R.J.M. Hudson. 1984. Integrated Acidification Study (ILWAS): A Mechanistic Ecosystem Analysis. Phil. Trans. R. Soc. Lond. B305, p. 409–425.

Goldstein, R.A., S.A. Gherini, C.T. Driscoll, R. April, C.L. Schofield, C.W. Chen. 1987. Lake-Watershed Acidification in the North Branch of the Moose River. Biogeochemistry 3:5–20.

Goldstein, R.A., C.W. Chen, and S.A. Gherini. 1985. The Integrated Lake-Watershed Acidification Study: Summary. Water, Air, and Soil Pollution. 26:327–337.

Linsley, R.K., M.A. Kohler, and J.L.H. Paulhus. 1975. Hydrology for Engineers, Second Edition, McGraw-Hill, New York.

Newton, R.M., J. Weintraub, and R. April. 1987. The Relationship Between Surface Water Chemistry and Geology of the North Branch of the Moose River. Biogeochemistry 3:21–35.

Peters, N.E., and C.T. Driscoll. 1987. Hydrogeologic Controls of Surface-Water in the Adirondack Region of New York State. Biogeochemistry 3:163–180.

Schofield, C.L., J.N. Galloway, and G.R. Hendry. 1985. Surface Water Chemistry in the ILWAS Basins. Water, Air, and Soil Pollution, 26:403–424.

Stumm, W. and J.J. Morgan. 1970. Aquatic Chemistry — An Introduction Emphasizing Chemical Equilibria in Natural Waters. John Wiley and Sons, Inc. pp. 1–583.

Stumm, W. and J.J. Morgan. 1981. Aquatic Chemistry — An Introduction Emphasizing Chemical Equilibria in Natural Waters. Second Edition. John Wiley and Sons, Inc. pp 1–780.